

Scoulerine promotes cytotoxicity and attenuates stemness in ovarian cancer by targeting PI3K/AKT/mTOR axis

FANG WANG¹
YANG ZHANG^{1*}
RUI PANG¹
SHAOHONG SHI¹
RAN WANG²

¹ Department of Gynaecology
Xuzhou Medical University
Affiliated Hospital of Lianyungang
Lianyungang, Jiangsu, China
222061

² Department of Clinical laboratory
Xuzhou Medical University
Affiliated Hospital of Lianyungang
Lianyungang, Jiangsu, China
222061

ABSTRACT

In women, ovarian cancer is a common gynecological cancer associated with poor prognosis, reoccurrence and chemoresistance. Scoulerine, a benzyloisoquinoline alkaloid, has been reported effective against several carcinomas. Thus, we investigated the impact of scoulerine on ovarian cancer cells (OVCAR3). Cell viability was assessed by MTT assay, migration was determined by Boyden Chamber assay, while the invasion was monitored by Boyden Chamber assay using the matrigel. The stemness properties of OVCAR3 cells were observed by tumorsphere assay. Epithelial to mesenchymal transition (EMT) and stemness-related protein markers were monitored by real-time PCR analysis and immunoblotting. Scoulerine inhibits the viability of OVCAR3 cells with the IC_{50} observed at $10 \mu\text{mol L}^{-1}$ after 48 h treatment. Scoulerine inhibited the colony-forming ability, migration and invasiveness of OVCAR3 cells in a dose-dependent fashion. Scoulerine treatment also drastically reduced the spheroid-forming ability of OVCAR3 cells. The mesenchymal and stemness-related markers like N-cadherin, vimentin, CD-44, Oct-4, Sox-2 and Aldh1A1 were downregulated, whereas the epithelial markers like E-cadherin and CD-24 were upregulated in scoulerine-treated cells. The upstream PI3K/Akt/mTOR-axis was downregulated in scoulerine-treated cells. We concluded that scoulerine successfully perturbs the cancerous properties of OVCAR3 cells by targeting the PI3K/Akt/mTOR axis. *In vivo* studies revealed a substantial decrease in tumor mass and volume after scoulerine treatment. Furthermore, scoulerine treatment was found to decrease oxidative stress factors in ovarian cancer mice model. Scoulerine is a potential anticancer agent against ovarian cancer and can be considered as a lead molecule for this malignancy, provided further investigations are performed.

Keywords: scoulerine, ovarian cancer, epithelial to mesenchymal transition, stemness, PI3K/Akt/mTOR axis

Accepted January 8, 2023
Published online January 9, 2023

Ovarian cancer is a common gynecological cancer associated with a poor prognosis (1). Nearly 200,000 women are diagnosed with ovarian cancer yearly worldwide. Among them, the chance of survival on a five-year scale is around 45 % (2). Epithelial ovarian cancer, one of

*Correspondence; e-mail: zhangyang19801027@njmu.edu.cn

its common subtypes, poses a major threat to patients due to high recurrence after the first line of treatment (3). Recurrence of ovarian cancer has been noted to be about 70 % (4). The cancer stage at diagnosis is one of the most important elements in evaluating a patient's likelihood of recurrence. The recurrence rate in stages 1, 2, 3 and 4 is 10, 30, 70 to 90 and 90 to 95 %, respectively, in ovarian cancer (4). Epithelial cells adhere to a higher degree on the basal membrane surface by intercellular adhesion complexes that are different from the mesenchymal ones, which are highly non-polar and possess higher cell-to-cell mobility (5). These two cell types are involved in the phenomenon known as epithelial-mesenchymal transition (EMT) by regulating several marker proteins (6, 7). EMT is also considered a promoter of metastasis (8). Transformations caused due to EMT result in cells acquiring mobility, a mesenchymal feature. Developing mesenchymal features eventually promotes the subpopulation of cancer stem cells (CSCs). The role of CSCs has been documented by many studies to be critical in the process of recurrence of ovarian cancer and also encourages chemoresistance development (9, 10). PI3K/AKT/mTOR signalling hyperactivation has been reportedly linked to cancer metastasis *via* CSCs and possible chemoresistance (11–13). Earlier reports have suggested regulation of this signalling cascade can be beneficial for controlling chemoresistance (14, 15). Though the standard option for treating ovarian cancer patients involves platinum-agent-based chemotherapy, there are a few more options like treatment with taxanes, hormonal therapy, *etc.* (16–18). However, the side effects of such therapies are inevitable (19, 20). Therefore, the search for novel anti-ovarian cancer agents is needed.

Scoulerine (SU) is an intermediate isoquinoline alkaloid plant metabolite found in *Croton flavens*, *Corydalis dubia* and *Corydalis cava* and is known to show antimetastatic effects against cancer cells (21). Scoulerine has been reported to possess anticancer properties (22, 23). Nevertheless, the anticancer properties of scoulerine against ovarian cancer and the associated molecular mechanisms have not been thoroughly investigated. The oncogenic potential of any cancer depends on EMT ability and its stem cell-like properties (24, 25). Cancer stem cells (CSCs) are characterized by CD-44/CD-24 surface markers, which gain their stem-like characteristics through EMT (26). Blocking the EMT in cancer cells also results in subsequent downregulation of stemness within cancer cells, reducing its metastatic potential (27). In the present study, we have aimed to investigate the effect of a natural compound, scoulerine, a benzyloisoquinoline alkaloid (Fig. 1a), on ovarian cancer cells (OVCAR3). Several reports have shown that scoulerine exhibits a broad spectrum of pharmacological activities, including antibacterial, antiemetic, anti-inflammatory and antitussive properties (28, 29). Reports have also suggested that scoulerine affects the activity of DNA topoisomerase I (30) and hence may be able to regulate gene expression. On the other hand, scoulerine is also known to show antiapoptotic and antiproliferative activities against cancer cells (22, 23). However, the antiproliferative role of scoulerine on ovarian cancer cells remains elusive. The present study aims to evaluate the possible effects of SU on the oncogenic properties, EMT and stemness of ovarian cancer cells and the upstream signalling cascade that may be involved.

EXPERIMENTAL

Materials

Scoulerine was procured from Herbest Bio-Tech, China (CAS 6451-73-6) (purity > 98 %). Human ovarian epithelial adenocarcinoma cells (OVCAR3; ATCC[®]HTB161TM) and HEK293;

ATCC®CRL-1573™) were obtained from the ATCC, USA. Antibodies, anti-GAPDH, anti-N-Cadherin, anti-E-Cadherin, anti-Vimentin, anti-CD44, anti-Oct-4, anti-Sox2, anti-Aldh1A1, anti-Akt and anti-p-Akt were obtained from Cell Signaling Technology (USA). While other antibodies, anti-CD24, anti-PI3K, anti-mTOR and anti-p-mTOR were purchased from Santa Cruz Biotechnology (USA). Clarity Western ECL substrate luminol assay kit was obtained from (BioRad Laboratories, Inc. Tumorsphere medium was obtained from Stem Cell Technologies. All chemicals are purchased from Sigma or stated accordingly.

Cell culture

Human ovarian epithelial adenocarcinoma cells (OVCAR3 and HEK293) were grown in DMEM supplemented with 10 % FBS and antibiotic (100 U mL⁻¹) in a CO₂ incubator.

Cell viability assay

The OVCAR3 and HEK293 (1 × 10⁴ cells mL⁻¹) cells were grown in a 96-well plate and subjected to scoulerine treatment for various time points (24 and 48 h). Cell viability was measured using the MTT assay. At the end of SU treatment, MTT stock solution of 5 mg mL⁻¹ concentration and volume 100 μL was supplemented to cells with 2 h of incubation at 37 °C. The formazan crystals then produced were dissolved using DMSO and after that, absorbance was measured at 570 nm using SpectraMax™ 340 microplate reader (Molecular Devices, USA) (31).

Colony formation assay

The OVCAR3 (1 × 10⁴ cells mL⁻¹) cells were treated with and incubated with or without SU (5 and 10 μmol L⁻¹) for 48 hours. After treatment, only the viable cells were transferred to 24 well plates at approximately 200 cells mL⁻¹ density and allowed to grow in normal culture conditions without SU for two weeks. After that, the colonies formed were stained with crystal violet and photographed using ECLIPSE Ti2 inverted microscope (NIKON). Colonies formed were quantified by dissolving the stained cells in methanol and the absorbance at 540 nm was measured using a SpectraMax™ 340 microplate reader (Molecular Devices) (32).

Trans-well migration and invasion assay

Boyden's chamber system was used to evaluate the migration of the ovarian OVCAR3 cells. Briefly, SU-treated and control OVCAR3 cells (10,000 cells) were added to the cell culture insert (Thermo, USA). On the other hand, to evaluate the invasiveness of OVCAR3 cells, a matrigel basement was used along with Boyden's chamber. The OVCAR3 (1 × 10⁴ cells mL⁻¹) cells were treated with or without SU (5 and 10 μmol L⁻¹) for 48 h. After treatment, only the viable cells were added to the cell culture insert (Thermo, USA) containing media or 100 μL Matrigel solutions (Corning, USA). The inserts were placed in 2 mL of serum-free culture media (SFCM) (negative control) and DMEM containing 10 % FBS as a chemo-attractant. The media was aspirated from the inserts after 24 hours and the membrane was washed three times in phosphate-buffered saline (PBS). The OVCAR3 cells were then subjected to crystal violet staining for 10 min. The cells were then rinsed in PBS to

remove any remaining stains. 24 hours after SU treatment, migration of cells was measured using ECLIPSE Ti2 inverted microscope (NIKON) at 100 × magnification. Image J software version 1.50 was used to quantify the wound region. After that, the remaining crystal violet stains in the plate were dissolved in 10 % acetic acid and the absorbance at 600 nm was measured using a SpectraMax™ 340 microplate reader (33).

Tumorsphere assay

The OVCAR3 (1×10^4 cells mL⁻¹) cells were treated with SU (5 and 10 μmol L⁻¹) for 48 h. After treatment, only the viable cells (1000 cells mL⁻¹) in single-cell suspension were grown in a tumorsphere medium containing heparin (4 μg mL⁻¹) and hydrocortisone (0.48 μg mL⁻¹) on ultralow attachment plates. Cultures were grown for 10 days to form the primary tumorspheres. The tumor spheres were counted and photographed using ECLIPSE Ti2 inverted microscope (NIKON). After capturing the images, the spheroids were again subjected to the single-cell suspension, reseeded in the complete tumorsphere medium and cultured for another 10 days to form the secondary spheroids. Image J software version 1.50 was used to measure the size of the spheres (34).

Quantitative RT-PCR study

Quantitative real-time PCR (qRT-PCR) was performed to analyze the expression of EMT (N-cadherin, E-cadherin, vimentin, CD-44 and CD-24) and CSC (Oct-4, Sox-2 and ALDH1A1) markers. Briefly, the TRIzol™ Reagent (Thermo Fisher Scientific) was used to extract the total RNA from tissues and cells according to the procedure described by the manufacturer. Isolated RNA was reverse-transcribed with the help of RevertAid's first-strand cDNA synthesis kit (Thermo Fisher Scientific). The RT-PCR was performed using SYBR Green PCR master mix (Takara, Japan) on Quant Studio 3.0 PCR system (Applied Biosystems). Experiments were conducted in triplicates. The relative expression levels were determined using the $2^{-\Delta\Delta CT}$ method with the human GAPDH gene as endogenous control. The primers used are mentioned in Table I.

Table I. Primer sets used for qRT-PCR analysis in this study

Set	Gene name	Forward primer (5'-3')	Reverse primer (5'-3')
1	N-cadherin	GCGTCTGTAGAGGCTTCTGG	GCCACTTGCCACTTTTCCTG
2	E-cadherin	GGTTTCTACAGCATCACCG	GCTTCCCCATTTGATGACAC
3	Vimentin	TGTCAAATCGATGTGGATGTTTC	TTGTACCATTCTTCTGCCTCCTG
4	CD-44	AGCAGCGGCTCCTCCAGTGA	CCCCTGGGGTGAATGTGTCT
5	CD-24	GACTCAGGCCAAGAAACGTC	CCTGTTTTCTTGCCACAT
6	Oct-4	GTTGATCCTCGGACCTGGCTA	GGTTGCCTCTACTCGGTTCT
7	Sox-2	CACATGAAGGAGCACCCGGATTAT	GTTTCATGTGCGCGTAACTGTCCAT
8	ALDH1A1	TGTTAGCTGATGCCGACTTG	TTCTTAGCCCGCTCAAACT
9	GAPDH	GAGAAGGCTGGGGCTCATT	AGTGATGGCATGGACTGTGG

Western blot analysis

The OVCAR3 (1×10^4 cells mL⁻¹) cells were treated with SU (5 and 10 μ mol L⁻¹) for 48 h and cellular proteins were extracted using Lysis buffer (Thermo, USA) after SU treatment. The concentration of protein was measured using the Bradford assay (35). The expression of the target protein was monitored using Western blot analysis. Primary and secondary antibodies were used at dilutions recommended by the manufacturer. Bands were visualized using the Clarity Western ECL substrate luminol assay kit and chemiluminescence was monitored using Chemidoc™ Gel Imaging System (Bio-Rad Laboratories, Inc.).

Experimental animals and in vivo study

Thirty BALB/c nude mice (6-week-old) were provided by the Vital River Laboratories, Animal Technology Co., Ltd. (China). All mice obtained were housed individually at 24 ± 1 °C temperature, under 60 % humidity and exposed to 12 h light/dark cycles. Free access was given to laboratory chow and water to all the mice *ad libitum*. The protocols on mice were conducted in accordance with the guidelines issued by the National Institutes of Health China. The animals were housed in sterilized cages ($n = 3$ per cage) and monitored under a standard laboratory environment (12 h:12 h day/night cycle, 22–23 °C, humidity 55–60 %). The mice were accustomed to the animal house conditions for five days before the start of the study. Approval for the present study was obtained from the Animal Care and Use Committee of the Xuzhou Medical University, China. SK-OV-3 Ovarian cells (1×10^6 cells/200 μ L) were subcutaneously inoculated into the flanks of female BALB/c nude mice to generate xenografts. Mice were assigned randomly to three groups of 10 each, sham, ovarian cancer model (model) and SU treatment (at 1, 2.5, 5 and 10 mg kg⁻¹ dose) groups. The drug was treated when the tumor volume came to 0.52 μ m³. Mice were sacrificed at the end of the treatment. The size of the tumor was measured using a digital caliper and the tumor volume was determined with the following formula: length (mm) \times width (mm) \times height (mm) \times 0.52.

Determination of oxidative factors

Blood samples were collected from the mice on day 16th day, and centrifuged at 4 °C for 15 min at 3,000 g to isolate the serum. The serum samples were stored at –80 °C for the determination of various factors by ELISA assay. The commercially available kits (Nanjing Jiancheng Biology Engineering Institute, China) were used to determine MDA (cat. no. A003-1), SOD (cat. no. A001-1), GSH (cat. no. A006-2) and GSH-PX (cat. no. A005) activities. Spectrophotometry was used for the measurement of absorbance at 450 nm wavelength using Microplate Reader (BioTek Instruments, Inc., USA).

Statistical analysis

The mean \pm standard deviation (SD) was used to express all data. Statistically significant differences between groups were established using the student's t-test for two-sample comparisons and the one-way ANOVA followed by Tukey's post hoc test for more than two-sample comparisons. Statistical analysis of various experimental data was done by using the GraphPad Prism 7 software (GraphPad Software, USA). $p < 0.05$ was considered statistically significant.

RESULTS AND DISCUSSION

Scoulerine inhibits the viability of OVCAR3 cells

The effect of SU on the proliferation of normal human embryonic HEK293 and human ovarian epithelial adenocarcinoma cells, OVCAR3, was studied by culturing the cells and

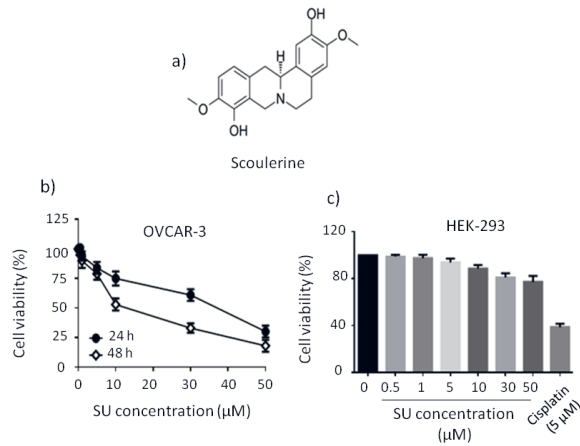


Fig. 1. a) Chemical structure of scoulerine; MTT assay for measuring cell viability of b) OVCAR3 and c) HEK-293 cells. Cells treated with cisplatin ($5 \mu\text{mol L}^{-1}$) were used as a positive control. All experiments were accomplished in triplicates and data are shown as mean \pm SD.

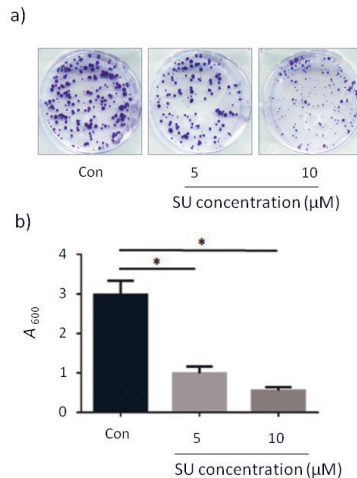


Fig. 2. a) Colony forming assay after treatment with 5 and 10 $\mu\text{mol L}^{-1}$ of scoulerine; b) graphical representation of inhibition of the colony formation ability of OVCAR3 by scoulerine. Colony quantification by spectrophotometric analysis is represented here. Experiments were accomplished in triplicates and data are shown as mean \pm SD. * $p < 0.05$ as compared to untreated cells.

treating them for 24 and 48 hours with various concentrations of SU (0–50 $\mu\text{mol L}^{-1}$) (Fig. 1a). The findings of the MTT assay revealed that SU substantially reduced OVCAR3 proliferation in a dose-dependent manner (Fig. 1b). After 24-hour incubation, the IC_{50} value was obtained at 40 $\mu\text{mol L}^{-1}$, whereas the IC_{50} value obtained after 48-hour incubation was 10 $\mu\text{mol L}^{-1}$. In addition, the IC_{50} concentration of SU did not affect the viability of HEK293 cells after 48-hour incubation (Fig. 1c).

According to our findings, scoulerine treatment considerably reduces cell viability in ovarian cancer cells (OVCAR3). However, scoulerine treatment shows little or no inhibitory impact on the HEK293 cell line. We may conclude that scoulerine specifically acts on ovarian cancer cells. Earlier studies reported that cancer cells like Caco-2 and HepG2 could be effectively inhibited from proliferating by scoulerine (22). Another recent study demonstrated that the tumour cell lines B16-F10, HepG2, K562 and HL-60 were sensitive to scoulerine extracted from the stems of *Xylopija laevigata* (36).

Scoulerine reduced the clonogenic property of OVCAR3 cells

The formation of viable colonies is one of the hallmark properties of cancer cells. We observed that SU decreased the colony-forming ability of OVCAR3 cells in a dose-dependent fashion (Fig. 2a). At 5 $\mu\text{mol L}^{-1}$ SU, the viable colonies were reduced to $60.3 \pm 5.6\%$, whereas, at a higher concentration of 10 $\mu\text{mol L}^{-1}$, the ability of colony formation by OVCAR3 cells was reduced further to approximately $78.3 \pm 2.2\%$, compared to control cells (Fig. 2b).

Scoulerine suppressed the migration and invasiveness of OVCAR3 cells

An assay involving Boyden's chamber was utilized to measure SU's impact on cell migration and invasiveness. Compared to untreated control, 5 $\mu\text{mol L}^{-1}$ SU substantially reduced OVCAR3 cell migration (Fig. 3a). The results indicated that when treated with

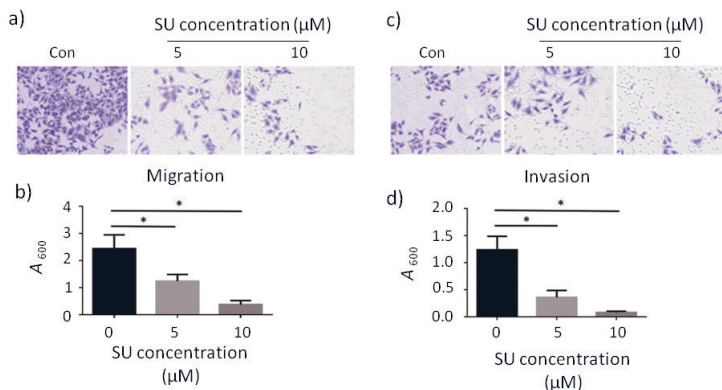


Fig. 3. a) Effect of scoulerine treatment on cell migration of OVCAR3 cells. Scale bar is 10 μm ; b) graphical representation of spectrophotometric data in a quantitative manner; c) effect of scoulerine treatment on the invasiveness of OVCAR3 cells. Scale bar is 10 μm ; d) graphical representation of spectrophotometric data in a quantitative manner. Experiments were performed in triplicates and data are shown as mean \pm SD. * $p < 0.05$ as compared to untreated cells.

5 $\mu\text{mol L}^{-1}$ SU, OVCAR3 cells lost their motility by $56.2 \pm 6.7\%$ and their invasiveness by $67.2 \pm 7.1\%$ compared to untreated cells. At a higher concentration of 10 $\mu\text{mol L}^{-1}$ SU, the motility and invasiveness of OVCAR3 cells decreased further to $82.6 \pm 4.5\%$ and $92.8 \pm 3.1\%$, respectively. Thus it may be concluded that SU significantly inhibited ovarian cancer cells' migration potential by $56.2 \pm 6.7\%$ ($p < 0.05$) (Fig. 3b) and invasiveness by $67.2 \pm 7.1\%$ ($p < 0.05$) compared to untreated cells (Fig. 3c,d).

Scoulerine reduced the sphere-forming ability of OVCAR3 cells

The sphere-forming assay was performed to identify the cancer stem cell (CSC) population of OVCAR3 cells. It was observed that the treatment of OVCAR3 cells with SU (5 and 10 $\mu\text{mol L}^{-1}$) significantly reduced both the size and numbers of primary and secondary spheres formed compared to the untreated cells (Fig. 4a). At 5 $\mu\text{mol L}^{-1}$ SU, primary spheres decreased by $69.6 \pm 5.3\%$ and secondary spheres by $91.5 \pm 2.7\%$ (Fig. 4b). On the other hand, at a higher dose (10 $\mu\text{mol L}^{-1}$ SU), the number of primary spheres decreased by $58.4 \pm 6.1\%$ and secondary spheres by $93.5 \pm 3.1\%$ (Fig. 4b). Thus, SU had a clear role in decreasing the cancer stem cell (CSC) like properties of ovarian cancer cells.

Downregulation of EMT and stem markers in scoulerine-treated OVCAR3 cells

Alteration of metastasis in cancer cells can be determined by changes in EMT markers. Changes to cell-to-cell adhesion receptors can be decreased by downregulating N-cadherin and vimentin and increasing the expression of E-cadherin (37). Compared to untreated

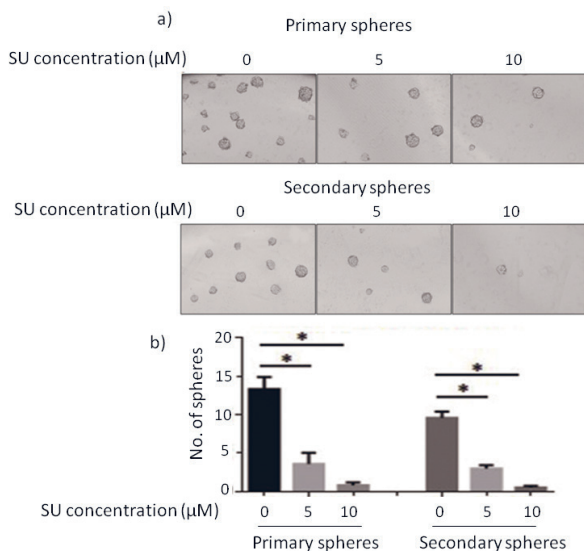


Fig. 4. a) Phase contrast microscopic image of primary and secondary spheroid formation. Scale bar is 10 μm ; b) graphical representation of primary and secondary spheroids formation ability in a quantitative manner. Experiments were performed in triplicates and data are shown as mean \pm SD. * $p < 0.05$ as compared to untreated cells.

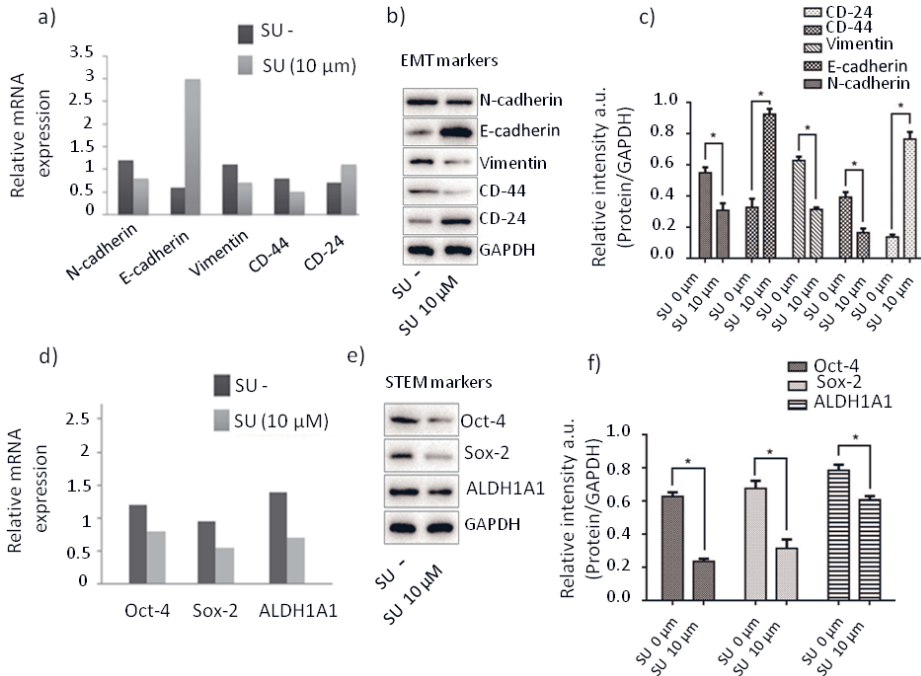


Fig. 5. a) mRNA and b) Western blot analyses for expression of E-cadherin, N-cadherin, Vimentin, CD-44 and CD-24; c) densitometric quantification of Western blot using ImageJ (NIH software); d) mRNA and e) Western blots analyses for expression of Oct-4, Sox-2 and Aldh1A1; f) densitometric quantification of Western blot using ImageJ (NIH software). Experiments were performed in triplicates and data are shown as mean \pm SD. * $p < 0.05$ as compared to untreated cells.

cells, SU-treated ovarian cancer cells showed dose-dependent upregulation of E-cadherin and downregulation of N-cadherin and vimentin (Fig. 5a–c). CD-44 downregulation is related to attenuating the malignant phenotype of various cancer cells (38). SU-treated OVCAR3 cells showed downregulation of CD-44 and upregulation of CD-24, indicating that SU blocks EMT of OVCAR3 cells and reduces its metastatic potential. Similarly, SU significantly reduced the stemness markers like Oct-4, Sox-2 and Aldh1A1 in OVCAR3 cells (Fig. 5d–f).

Scoulerine treatment was reported to reduce clonogenic ability, migration potential, invasiveness and tumor spheroid-forming ability of ovarian cancer cells. As these properties relate to the reduction of metastatic potential of cancer cells, we investigated the EMT and stemness markers of scoulerine-treated OVCAR3 cells. To our expectations, we found a dose-dependent overexpression of E-cadherin, while the expression of N-cadherin and vimentin were downregulated. Furthermore, CD-44 was found to be downregulated and CD-24 to be upregulated. These expression levels suggest that scoulerine helps block the EMT of OVCAR3 cells, therefore helping reduce metastasis. Stem cell-like properties of OVCAR3 cells were decreased as the expression of stemness markers, Oct-4, Sox-2 and Aldh1A1, got downregulated on treatment with scoulerine.

Downregulation of PI3K/Akt/mTOR signaling pathway in scoulerine-treated OVCAR3 cells

Alteration in CD-44 expression is mainly related to altered expression of the PI3K/AKT signalling cascade. Hence we investigated whether SU affected the PI3K/AKT/mTOR pathway in OVCAR3 cells by measuring the levels of p-AKT, p-mTOR and PI3K (P85) in OVCAR3 cells. SU significantly reduced the PI3K (P85), p-AKT and p-mTOR levels while keeping AKT and mTOR protein expressions unchanged (Fig. 6a,b). Thus the results indicate that SU may target the upstream PI3K/AKT signalling cascade in OVCAR3 cells.

Alterations in EMT and stemness can be related to upstream PI3K/AKT/mTOR pathway downregulation (39). The same was found in the case of scoulerine-treated OVCAR3 cells. A dose-dependent downregulation of p-AKT, p-mTOR and PI3K was observed, whereas the AKT and mTOR levels were unchanged. This indicates that scoulerine acts as a regulator of the PI3K/AKT/mTOR pathway, which blocks the EMT and stem cell-like properties of ovarian cancer cells. Therefore, these findings indicate that scoulerine decreased cell viability and metastatic potential of the OVCAR3 cells by acting on PI3K/AKT/mTOR axis.

In vivo inhibition of tumor mass and volume in scoulerine-treated ovarian cancer mice model

In vivo studies on xenografted models of mice were performed to unveil *in vivo* anti-cancer potential of scoulerine. The results indicated potential suppression of ovarian cancer in a dose-dependent manner. The tumor mass in controls was nearly 2.1 g. After the application of scoulerine, the tumor mass decreased from 2.1 to about 0.7 g at 10 mg kg⁻¹ of scoulerine (Fig. 7a), signifying substantial dose-dependent mass loss of tumor mass after drug treatment. Next, investigations were performed on tumor volume and the results implied decrease in tumor volume after treatment with scoulerine. The control tumor

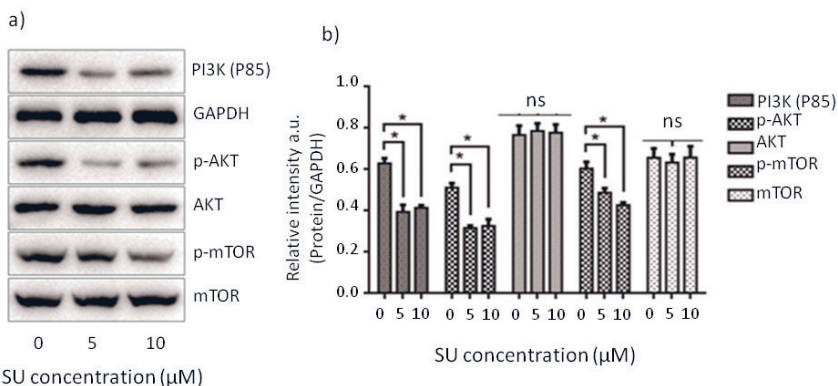


Fig. 6. a) Western blot analysis for expression of PI3k (p85), AKT, pAKT, mTOR, p-mTOR and GAPDH proteins; b) densitometric quantification of Western blot using ImageJ (NIH software). Experiments were performed in triplicates and data are shown as mean \pm SD. * $p < 0.05$ as compared to untreated cells.

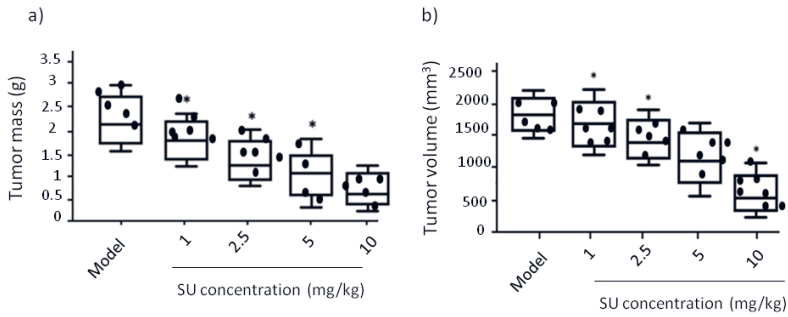


Fig. 7. a) *In vivo* effect of scoulerine on ovarian tumor mass in xenografted models of mice at represented doses; b) *in vivo* effect of scoulerine on ovarian tumor volume in xenografted models of mice at represented doses. Data from three distinct experiments are stated as mean \pm standard deviation (* $p < 0.05$).

volume was about 1800 mm³, which was reduced to about 1100 mm³ at 5 mg kg⁻¹ of drug dose. On further increasing the maslinic acid dose (10 mg kg⁻¹), the tumor volume shortened to almost 600 mm³ (Fig. 7b).

Scoulerine decreased oxidative stress in ovarian cancer mice model

In the ovarian cancer mice model the activities of SOD, CAT and GSH were lower in serum compared to treated mice groups. The MDA level in ovarian cancer mice model

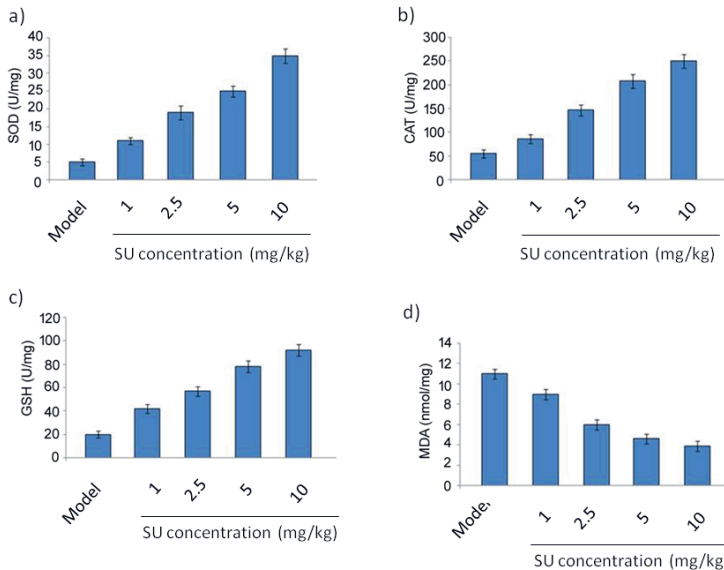


Fig. 8. Effect of scoulerine on oxidative stress factors in ovarian cancer mice model. The effect of 1, 2.5, 5 and 10 mg kg⁻¹ scoulerine in a mice model on: a) SOD; b) CAT and c) GSH activities; d) the level of MDA was also determined.

serum was higher compared to treated mice groups. Scoulerine treatment alleviated SOD, CAT and GSH activities significantly in the mice model at doses of 1, 2.5, 5 and 10 mg kg⁻¹ (Fig. 8a–d). Moreover, the MDA level was decreased after treatment with scoulerine at doses of 1, 2.5, 5 and 10 mg kg⁻¹ in a dose-based manner.

CONCLUSIONS

In summary, our results showed that scoulerine treatment induces cytotoxicity, inhibits colony-forming ability, migration and invasiveness, and attenuates stemness in ovarian cancer cells by targeting PI3K/AKT/mTOR axis. Scoulerine treatment inhibited tumor growth and volume in the ovarian cancer mice model by targeting oxidative response. Further, detailed knockdown approaches would shed more light on the molecular mechanism of scoulerine in ovarian cancer.

Abbreviations. – CSCs – cancer stem cells, DMEM – Dulbecco’s Modified Eagle Medium, ECL – enhanced chemiluminescence, EMT – epithelial-mesenchymal transition, PBS – phosphate-buffered saline, SU – scoulerine.

Acknowledgments. – The authors are very grateful for support from Xuzhou Medical University Affiliated Hospital of Lianyungang, Haizhou District, Lianyungang, Jiangsu, China.

Conflicts of interest – The authors declare no conflict of interest.

Authors contributions – Conceptualization, F.W. and Y.Z.; methodology R.P. and S.S; analysis R.W.; investigation, F.W. and R.P.; writing, original draft preparation, Y.Z.; writing, review and editing, Y.Z. and S.S. All authors have read and agreed to the published version of the manuscript.

REFERENCES

1. Y. Zhang, G. Luo, M. Li, P. Guo, Y. Xiao, H. Ji and Y. Hao, Global patterns and trends in ovarian cancer incidence: age, period and birth cohort analysis, *BMC Cancer* 19(1) (2019) Article ID 984 (14 pages); <https://doi.org/10.1186/s12885-019-6139-6>
2. B. M. Reid, J. B. Permuth and T. A. Sellers, Epidemiology of ovarian cancer: a review, *Cancer Biol. Med.* 14(1) (2017) 9–32; <https://doi.org/10.20892/j.issn.2095-3941.2016.0084>
3. M. A. Amaya Padilla, M. Binju, G. Wan, Y. S. Rahmanto, P. Kaur and Y. Yu, Relationship between ovarian cancer stem cells, epithelial mesenchymal transition and tumour recurrence, *Cancer Drug Resist.* 2(4) (2019) 1127–1135; <https://doi.org/10.20517/cdr.2019.76>
4. K. Ushijima, Treatment for recurrent ovarian cancer at first relapse, *J. Oncol.* 2010 (2010) 1–7; <https://doi.org/10.1155/2010/497429>
5. H. Aclouque, M. S. Adams, K. Fishwick, M. Bronner-Fraser and M. A. Nieto, Epithelial-mesenchymal transitions: the importance of changing cell state in development and disease, *J. Clin. Invest.* 119(6) (2009) 1438–1449; <https://doi.org/10.1172/JCI38019>
6. F. Guo, B. C. Parker Kerrigan, D. Yang, L. Hu, I. Shmulevich, A. K. Sood, F. Xue and W. Zhang, Post-transcriptional regulatory network of epithelial-to-mesenchymal and mesenchymal-to-epithelial transitions, *J. Hematol. Oncol.* 7 (2014) Article ID 19 (11 pages); <https://doi.org/10.1186/1756-8722-7-19>
7. M. Zeisbergand, E. G. Neilson, Biomarkers for epithelial-mesenchymal transitions, *J. Clin. Invest.* 119(6) (2009) 1429–1437; <https://doi.org/10.1172/JCI36183>
8. M. Scimeca, C. Antonacci, D. Colombo, R. Bonfiglio, O. C. Buonomo and E. Bonanno, Emerging prognostic markers related to mesenchymal characteristics of poorly differentiated breast cancers, *Tumour Biol.* 37(4) (2016) 5427–5435; <https://doi.org/10.1007/s13277-015-4361-7>

9. K. D. Steffensen, A. B. Alvero, Y. Yang, M. Waldstrom, P. Hui, J. C. Holmberg, D. A. Silasi, A. Jakobsen, T. Rutherford and G. Mor, Prevalence of epithelial ovarian cancer stem cells correlates with recurrence in early-stage ovarian cancer, *J. Oncol.* **2011** (2011) Article ID 620523 (13 pages); <https://doi.org/10.1155/2011/620523>
10. Z. Pieterse, M. A. Amaya-Padilla, T. Singomat, M. Binju, B. D. Madjid, Y. Yu and P. Kaur, Ovarian cancer stem cells and their role in drug resistance, *Int. J. Biochem. Cell Biol.* **106** (2019) 117–126; <https://doi.org/10.1016/j.biocel.2018.11.012>
11. P. Liu, H. Cheng, T. M. Roberts and J. J. Zhao, Targeting the phosphoinositide 3-kinase pathway in cancer, *Nat. Rev. Drug Discov.* **8** (2009) 627–44; <https://doi.org/10.1038/nrd2926>
12. C. Gewinner, Z. C. Wang, A. Richardson, J. Teruya-Feldstein, D. Ettemadmoghadam, D. Bowtell, J. Barretina, W. M. Lin, L. Rameh, L. Salmena, P. P. Pandolfi and L. C. Cantley, Evidence that inositol polyphosphate 4-phosphatase type II is a tumor suppressor that inhibits PI3K signaling, *Cancer Cell* **16**(2) (2009) 115–125; <https://doi.org/10.1016/j.ccr.2009.06.006>
13. X. Tan, S. Chen, J. Wu, J. Lin, C. Pan, X. Ying, Z. Pan, L. Qiu, R. Liu, R. Geng and W. Huang, PI3K/AKT-mediated upregulation of WDR5 promotes colorectal cancer metastasis by directly targeting ZNF407, *Cell Death Dis.* **8**(3) (2017) Article ID e2686 (12 pages); <https://doi.org/10.1038/cddis.2017.111>
14. S. D. Westfalland, M. K. Skinner, Inhibition of phosphatidylinositol 3-kinase sensitizes ovarian cancer cells to carboplatin and allows adjunct chemotherapy treatment, *Mol. Cancer Ther.* **4**(11) (2005) 1764–177; <https://doi.org/10.1158/1535-7163.mct-05-0192>
15. H. J. Choi, J. H. Heo, J. Y. Park, J. Y. Jeong, H. J. Cho, K. S. Park, S. H. Kim, Y. W. Moon, J. S. Kim and H. J. An, A novel PI3K/mTOR dual inhibitor, CMG002, overcomes the chemoresistance in ovarian cancer, *Gynecol. Oncol.* **153**(1) (2019) 135–148; <https://doi.org/10.1016/j.ygyno.2019.01.012>
16. D. K. Armstrong, B. Bundy, L. Wenzel, H. Q. Huang, R. Baergen, S. Lele, L. J. Copeland, J. L. Walker and R. A. Burger, Intraperitoneal cisplatin and paclitaxel in ovarian cancer, *N. Engl. J. Med.* **354**(1) (2006) 34–43; <https://doi.org/10.1056/NEJMoa052985>
17. M. Cristea, E. Han, L. Salmon and R. J. Morgan, Review: Practical considerations in ovarian cancer chemotherapy, *Ther. Adv. Med. Oncol.* **2**(3) (2010) 175–187; <https://doi.org/10.1177/1758834010361333>
18. D. Jelovac and D. K. Armstrong, Recent progress in the diagnosis and treatment of ovarian cancer, *CA Cancer J. Clin.* **61**(3) (2011) 183–203; <https://doi.org/10.3322/caac.20113>
19. D. Cella, A. Peterman, S. Hudgens, K. Webster and M. A. Socinski, Measuring the side effects of taxane therapy in oncology: the functional assesment of cancer therapy-taxane (FACT-taxane), *Cancer* **98**(4) (2003) 822–831; <https://doi.org/10.1002/cncr.11578>
20. F. Steger, M. G. Hautmann and O. Kolbl, 5-FU-induced cardiac toxicity--an underestimated problem in radiooncology?, *Radiat. Oncol.* **7** (2012) Article ID 212 (4 pages); <https://doi.org/10.1186/1748-717X-7-212>
21. J. H. Schrittwieser, V. Resch, S. Wallner, W. D. Lienhart, J. H. Sattler, J. Resch, P. Macheroux and W. Kroutil, Biocatalytic organic synthesis of optically pure (S)-scoulerine and berbine and benzyloquinoline alkaloids, *J. Org. Chem.* **76**(16) (2011) 6703–6714; <https://doi.org/10.1021/jo201056f>
22. K. Habartova, R. Havelek, M. Seifrtova, K. Kralovec, L. Cahlikova, J. Chlebek, E. Cermakova, N. Mazankova, J. Marikova, J. Kunes, L. Novakova and M. Rezacova, Scoulerine affects microtubule structure, inhibits proliferation, arrests cell cycle and thus culminates in the apoptotic death of cancer cells, *Sci. Rep.* **8**(1) (2018) Article ID 4829 (14 pages); <https://doi.org/10.1038/s41598-018-22862-0>
23. J. Tian, J. Mo, L. Xu, R. Zhang, Y. Qiao, B. Liu, L. Jiang, S. Ma and G. Shi, Scoulerine promotes cell viability reduction and apoptosis by activating ROS-dependent endoplasmic reticulum stress in colorectal cancer cells, *Chem. Biol. Interact.* **327** (2020) Article ID 109184; <https://doi.org/10.1016/j.cbi.2020.109184>
24. J. Roche, The epithelial-to-mesenchymal transition in cancer, *Cancers (Basel)* **10**(2) (2018) Article ID 52 (4 pages); <https://doi.org/10.3390/cancers10020052>

25. D. Ribatti, R. Tamma and T. Annese, Epithelial-mesenchymal transition in cancer: A historical overview, *Transl. Oncol.* **13**(6) (2020) Article ID 100773 (9 pages); <https://doi.org/10.1016/j.tranon.2020.100773>
26. Z. Yu, T. G. Pestell, M. P. Lisanti and R. G. Pestell, Cancer stem cells, *Int. J. Biochem. Cell Biol.* **44**(2) (2012) 2144–2151; <https://doi.org/10.1016/j.biocel.2012.08.022>
27. S. Floor, W. C. van Staveren, D. Larsimont, J. E. Dumont and C. Maenhaut, Cancer cells in epithelial-to-mesenchymal transition and tumor-propagating-cancer stem cells: distinct, overlapping or same populations, *Oncogene* **30**(46) (2011) 4609–4621; <https://doi.org/10.1038/onc.2011.184>
28. P. Wangchuk, T. Sastraruji, M. Taweechotipatr, P. A. Keller and S. G. Pyne, Anti-inflammatory, anti-bacterial and anti-acetylcholinesterase activities of two isoquinoline alkaloids-scoulerine and cheilanthesifoline, *Nat. Prod. Commun.* **11**(12) (2016) 1801–1804; <https://doi.org/10.1177/1934578X1601101207>
29. P. Wangchuk, P. A. Keller, S. G. Pyne, A. C. Willis and S. Kamchonwongpaisan, Antimalarial alkaloids from a Bhutanese traditional medicinal plant *Corydalis dubia*, *J. Ethnopharmacol.* **143**(1) (2012) 310–313; <https://doi.org/10.1016/j.jep.2012.06.037>
30. X. Cheng, D. Wang, L. Jiang and D. Yang, DNA topoisomerase I inhibitory alkaloids from *Corydalis saxicola*, *Chem. Biodivers.* **5**(7) (2008) 1335–1344; <https://doi.org/10.1002/cbdv.200890121>
31. A. Das, A. Bhattacharya, S. Chakrabarty, A. Ganguli and G. Chakrabarti, Smokeless tobacco extract (STE)-induced toxicity in mammalian cells is mediated by the disruption of cellular microtubule network: a key mechanism of cytotoxicity, *PLoS One* **8**(7) (2013) Article ID e68224 (12 pages); <https://doi.org/10.1371/journal.pone.0068224>
32. N. A. Franken, H. M. Rodermond, J. Stap, J. Haveman and C. van Bree, Clonogenic assay of cells in vitro, *Nat. Protoc.* **1**(5) (2006) 2315–2319; <https://doi.org/10.1038/nprot.2006.339>
33. J. Pijuan, C. Barcelo, D. F. Moreno, O. Maiques, P. Siso, R. M. Marti, A. Macia and A. Panosa. In vitro cell migration, invasion and adhesion assays: From cell imaging to data analysis, *Front. Cell Dev. Biol.* **7** (2019) Article ID 107 (16 pages); <https://doi.org/10.3389/fcell.2019.00107>
34. I. Haque, A. Ghosh, S. Acup, S. Banerjee, K. Dhar, A. Ray, S. Sarkar, S. Kambhampati and S. K. Banerjee, Leptin-induced ER-alpha-positive breast cancer cell viability and migration is mediated by suppressing CCN5-signaling via activating JAK/AKT/STAT-pathway, *BMC Cancer* **18**(1) (2018) Article ID 99 (14 6)
35. A. Das, S. Chakrabarty, D. Choudhury and G. Chakrabarti, 1,4-Benzoquinone (PBQ) induced toxicity in lung epithelial cells is mediated by the disruption of the microtubule network and activation of caspase-3, *Chem. Res. Toxicol.* **23**(6) (2010) 1054–1066; <https://doi.org/10.1021/tx1000442>
36. L. R. Menezes, C. O. Costa, A. C. Rodrigues, F. R. Santo, A. Nepel, L. M. Dutra, F. M. Silva, M. B. Soares, A. Barison, E. V. Costa and D. P. Bezerra, Cytotoxic alkaloids from the stem of *Xylopia laevigata*, *Molecules* **21**(7) 2016 Article ID 890 (10 pages); <https://doi.org/10.3390/molecules21070890>
37. R. Y. Huang, P. Guilford and J. P. Thiery, Early events in cell adhesion and polarity during epithelial-mesenchymal transition, *J. Cell Sci.* **125**(Pt 19) (2012) 4417–4422; <https://doi.org/10.1242/jcs.099697>
38. H. Xu, Y. Tian, X. Yuan, H. Wu, Q. Liu, R. G. Pestell and K. Wu, The role of CD44 in epithelial-mesenchymal transition and cancer development, *Onco Targets Ther.* **8** (2015) 3783–3792; <https://doi.org/10.2147/OTT.S95470>
39. Z. Zou, T. Tao, H. Li and X. Zhou, mTOR signaling pathway and mTOR inhibitors in cancer: progress and challenges, *Cell Biosci.* **10** (2020) Article ID 31 (11 pages); <https://doi.org/10.1186/s13578-020-00396-1>